

## INVESTIGATIONS OF METAL GASKETS FOR HIGH-PRESSURE JOINTS

Andrzej Trojnecki, Maciej Krasieński, Bogdan Szybiński

Cracow University of Technology  
Department of Mechanical Engineering  
Jana Pawła II Avenue 37, 31-864 Krakow, Poland  
tel.: + 48 12 374 33 06, fax: + 48 12 374 33 60  
e-mail: [atroj@mech.pk.edu.pl](mailto:atroj@mech.pk.edu.pl)  
[mkr@mech.pk.edu.pl](mailto:mkr@mech.pk.edu.pl), [boszyb@mech.pk.edu.pl](mailto:boszyb@mech.pk.edu.pl)

### Abstract

The article deals with the stress-strain analysis and investigations of operating properties of metal high-pressure gaskets. The simplified analytical approach is applied in the examinations of wave-ring gasket and lens-ring gasket. A cylindrical shell of constant mean thickness is introduced to simulate the gaskets. It is assumed that the shell is simply supported at the inner surfaces of the gasket seats. The influence of certain geometric, material and assembly parameters on the strength and leak-tightness of the closures is analytically investigated. Certain selected parameters of the closure are examined versus applied operating pressure for the assumed materials of the gasketed members and fixed several another data of the gaskets. The analysis is carried out in dimensionless variables in order to generalize the results. The region of admissible solutions for the gaskets parameters such as dimensions, applied assembly requirements and operating pressure is determined. The static tensile tests were carried out to determine the real mechanical properties of materials applied for the gaskets and the seats. The analytical solutions are verified by FEM calculations, which take into account the hardening of the material, friction at the surfaces and contact effects. Theoretical considerations are illustrated by numerical examples and compared with the experimental results obtained under assembly conditions with no operating pressure applied to the closures. Some conclusions may be recommended in design procedures of the high-pressure closures with metal gaskets.

**Keywords:** high-pressure closures, metal gaskets, stress-strain analysis, leak tightness, FEM

### 1. Introduction

Modern power installations and advanced chemical equipment, usually operating at extremely high pressures, require reliable and hardwearing sealing systems. Metal gaskets are sometimes used to seal the heads of reactors and boilers, pipe connections and additional accessories. Metal gaskets give satisfactory sealing service, and furthermore, they are chemically resistant, moisture-proof and heat stable. There are many types of sealing closures with metal gaskets.

The present article deals with the stress-strain analysis and investigations of operating properties of *wave-ring gasket* and *lens-ring gasket*. These gaskets are often used in sealing systems; nevertheless, they are not adequately presented in technical literature. Actually, no procedures exist which can be adopted in design projects of the closures. In each individual case of technical application, a set of complex and time-consuming calculations of strength and leak tightness must be carried out. The assembly conditions and technical inspection requirements must be determined. The aim of the article is numerical and experimental verification of certain simple computational models of the joints, which could be applied to develop engineering formulas to determine geometry, material properties, assembly and operating parameters of the closures.

### 2. Engineering examples and service conditions of the sealings

An engineering example of the joint with wave-ring gasket is shown in Fig. 1a. The closure is successfully applied in the heavy-duty chemical installation working at the pressure of 200 MPa.

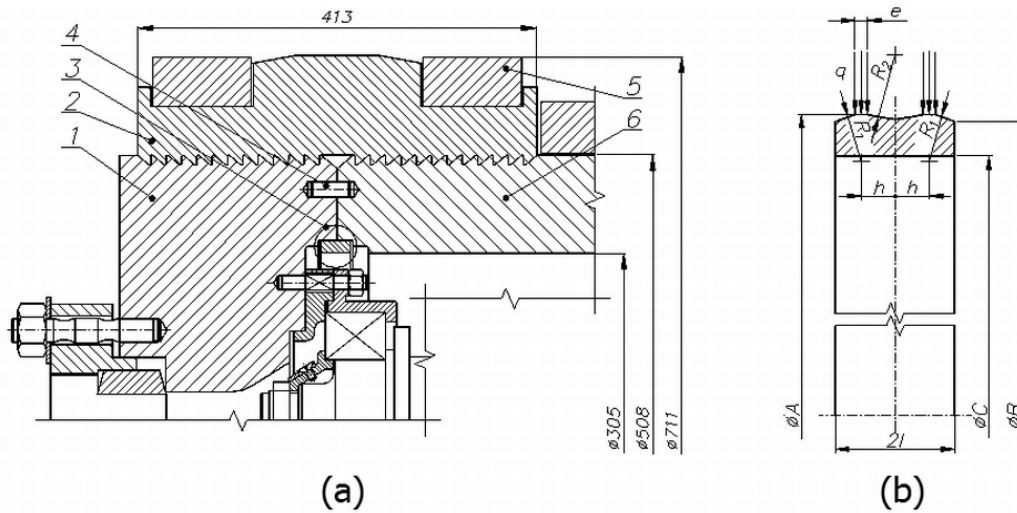


Fig. 1. Closure with the wave-ring gasket: (a) Engineering example of the joint between the vessel wall and reactor head. Specification: 1 – head, 2 – sectional clamping rings, 3 – gasket, 4 – locating pin, 5 – grips, 6 – cylindrical shell; (b) Geometry of the wave-ring gasket and the distribution of the assembly stress  $q$  at the contact surface

The yield stress of the wave-ring gasket material must be significantly lower than that of the seat material to ensure the proper effectiveness of the joint. The gasket is made slightly oversized, so that an interference fit is obtained in the seat at the diameter  $\phi A$ . Under assembly conditions, the initial contact pressure  $q$  appears at the portion  $e$  of a wave surface due to the assembly interference, thus making the initial seal just before the operating pressure  $p$  is applied (Fig. 1b). The working pressure is exerted on the entire inner surface, forcing a seal on the two outer radii.

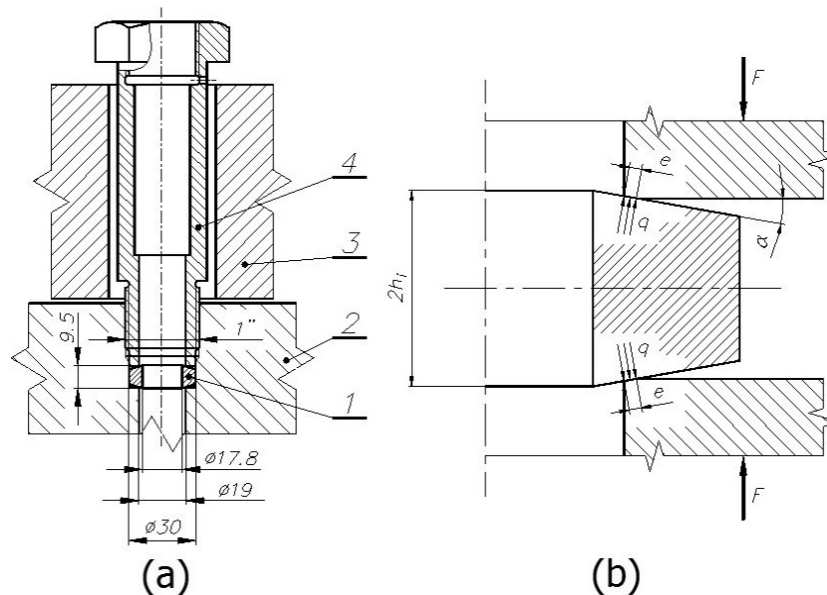


Fig. 2. Closure with the lens-ring gasket: (a) Engineering example of the joint used to seal the housing of the electrode. Specification: 1 – gasket, 2 – reactor vessel, 3 – clamping ring, 4 – screw joint; (b) Geometry of the lens-ring gasket and the distribution of the assembly stress  $q$  at the contact surface

The closures with lens-ring gaskets are usually used to seal small openings (Fig. 2a). In this case, the working sealing surfaces of the gasket must be of high hardness. When assembling a closure, a sufficient force  $F$  is applied in order to ensure that both relatively softer segments of the sharp-edged seat deform at the width  $e$ , and initial pressure  $q$  is obtained there (Fig. 2b). Internal operating pressure  $p$  acting on the members of the closure generates a decrease of the

assembly force  $F$  and a relevant decrease of initial pressure  $q$ . On the other hand, under the pressure  $p$ , the contact pressure  $q$  increases because the gasket expands, as its stiffness is lower than that of seats.

### 3. Simplified analytical solutions of the gaskets

Several analytical models of the wave-ring gasket and of the lens-ring gasket were created and investigated in [1, 3] with the aim of selecting the simplest and most effective one but sufficiently precise, which could be applied in the engineering approach.

The waviness of the wave-ring gasket-working surface is small (Fig. 1b). The maximum relative difference of the thickness for the considered gasket is less than 27.5%. For the continuous change in the thickness, the gasket may be replaced by a cylindrical shell of a constant thickness  $t$  and of a mean radius  $r$ , where  $t$  is defined as an arithmetic average of the three extreme values of the gasket thickness. The analytical calculations verified by FEM modelling lead to the conclusion that the influence of external parts of the gasket outside of the supports (broken line in Fig. 3) is negligible. The analytical investigations of the gasket are then based on a simple *shell model* of length  $2h$ , simply supported around the circumference at a contact with the seat. The spacing of the supports is  $2h$  (Fig. 3).

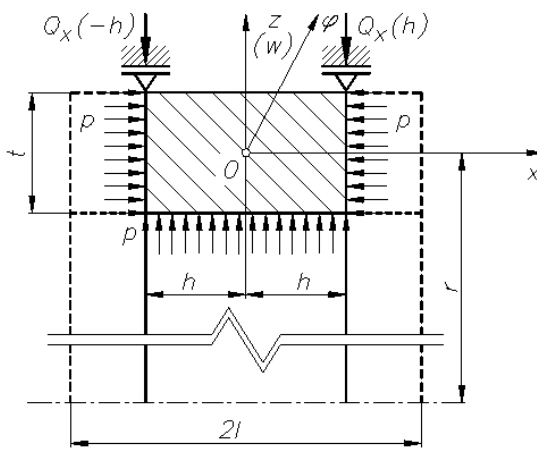


Fig. 3. Simplified model of the wave-ring gasket

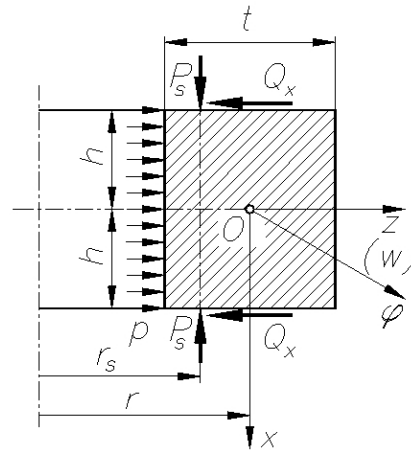


Fig. 4. Simplified model of the lens-ring gasket

Geometry and loading applied in the analysis of the lens-ring gasket are presented in Fig. 4. The hardened sealing surfaces of the gasket are sloped to the axis of the closure with a certain small angle  $\alpha$  (Fig. 2b). The shell of rectangular cross-section seems to be an adequate model of this gasket of real trapezoidal cross-section. Such an approach introduces a certain small error to the calculations but significantly simplifies the solution of the problem.

The simple shell model is then adopted to simulate both gaskets. The applied approach and permissible simplifications depend in the elastic shell theory on the geometric proportions of the analysed element. Following the estimation given in [8] the shells must be considered as “short” and of “mean thickness”. In this case, the gaskets must be solved on the basis of the *bending shell theory* and some terms in the differential equation of deflection could not be neglected. Moreover, it is assumed that except a small region in the vicinity of supports the shells are purely elastic.

Under the assumptions as for the *cylindrical axisymmetric shell* of mean thickness  $t$ , of mean radius  $r$  and of small radial deflections  $w$  with respect to the thickness  $t$ , the differential equation of deflection takes well-known form [8]:

$$\frac{d^4 w}{dx^4} + a \frac{d^2 w}{dx^2} + b^4 w = c, \quad (1)$$

where  $a = \nu/r^2$ ,  $b = \sqrt[4]{12(1-\nu^2)/r^2t^2}$ ,  $c = 12p(1-\nu^2)/Et^3$  and  $\nu$  and  $E$  stand for the Poisson's ratio and Young's modulus, respectively. The solution of equation (1) may be written as:

$$w(x) = C_1 \cosh\left(\frac{b}{\sqrt{2}}x\right) \cos\left(\frac{b}{\sqrt{2}}x\right) + C_2 \sinh\left(\frac{b}{\sqrt{2}}x\right) \sin\left(\frac{b}{\sqrt{2}}x\right) + w_p, \quad (2)$$

where  $w_p = pr^2/Et = \text{const}$ . Because of the symmetry with respect to the  $z$ -axis, only two constants of integration  $C_1$  and  $C_2$  appear in the solution (2). They can be determined from the boundary conditions as for the simply supported shell for the wave-ring gasket (Fig. 3) or from the known bending moments  $P_s(r-r_s)$  and shear forces  $Q_x$  at the outermost cross-sections for the lens-ring gasket (Fig. 4). The principal stresses  $\sigma_z$ ,  $\sigma_\phi$  and  $\sigma_x$  may be easily determined next in terms of shell parameters modelling the gaskets and of the operating pressure  $p$ . The maximum equivalent *Huber-Mises-Hencky* (H-M-H) stress equals

$$\sigma_{eq} = \sqrt{\sigma_z^2 + \sigma_\phi^2 + \sigma_x^2 - \sigma_z\sigma_\phi - \sigma_\phi\sigma_x - \sigma_x\sigma_z} \quad (3)$$

and appears at the inner cylindrical surface of the mid-section.

#### 4. Numerical modelling of the closures

In the present article, the ANSYS® code is used to solve the problem and to get the strain and stress distributions. The considered problem concerns the contact of two deformable bodies and belongs to the class of *flexible-to-flexible* contact [7]. The high accuracy of numerical results is provided by application of 8-node *quadrilateral axisymmetric finite elements*, which are well suited for irregular meshes and tasks with elastic and plastic deformations. These finite elements are accompanied with the *contact elements* introduced on lines where the contact is expected.

Tab. 1. Mechanical properties of materials of the closure members

Element	Material	$E \times 10^{-5}$ [MPa]	$R_{0.05}$ [MPa]	$R_{0.2}$ [MPa]	$R_m$ [MPa]	$\varepsilon_{0.05}$ [%]	$\varepsilon_{0.2}$ [%]	$\varepsilon_{\max}$ [%]
Wave-ring gasket	25CrMo4 (N)	2.014	253.59	260.30	523.38	0.185	0.359	15.34
Lens-ring gasket	40H2MF (T)	2.065	565.98	705.43	968.00	0.323	0.542	2.412
Seats	42CrMo4 (T)	2.064	809.12	812.46	918.50	0.460	0.711	8.802

The high assembly forces cause plastic deformations at the contact regions. Physical nonlinearity of materials must be then taken into account. The gaskets and the seats are made of materials which mechanical properties were experimentally verified in the *uniaxial tensile tests* (Tab. 1). The character of nominal load-deflection curves beyond the yield point suggests the parabolic approximations of  $\sigma = f(\varepsilon)$  relationships. The parabola containing the point of coordinates  $[\varepsilon_{0.2}, R_{0.2}]$  and reaching its maximum at the point  $[\varepsilon_{\max}, R_m]$  is applied to describe the materials. For the detailed numerical calculations, the parabola is replaced by several segments of different slope but of equal length in the orthogonal projection at the  $\varepsilon$  axis. Such an approximation enables direct introduction of the nonlinear material properties into the software module ANSYS®. Moreover, it is assumed that the relationship between the equivalent stress and equivalent strain under complex stress states  $\sigma_{eq} = f(\varepsilon_{eq})$  is the same as the stress-strain relationship under uniaxial tensile loading  $\sigma = f(\varepsilon)$  [8].

Several numerical tests based on the *trial-and-error method* have been carried out to get the final mesh of the closures. The compromise between the calculation time and the approximation

error has been established as the criterion for the choice of the element size in the contact area. The approximation error is based on the comparison between the maximum absolute value of the radial stress  $\sigma_{z \max}$ , and the maximum contact pressure  $q_{\max}$  accepts the mesh for which the discrepancy is less than 5% for each load step [4].

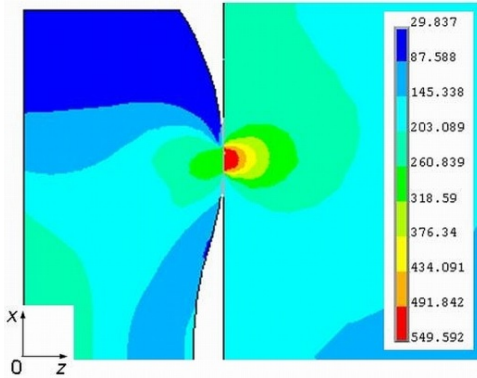


Fig. 5. Stress  $\sigma_{eq}$  for  $\delta = 1.0\%$  under the loading  $p = 100$  MPa (wave-ring gasket)

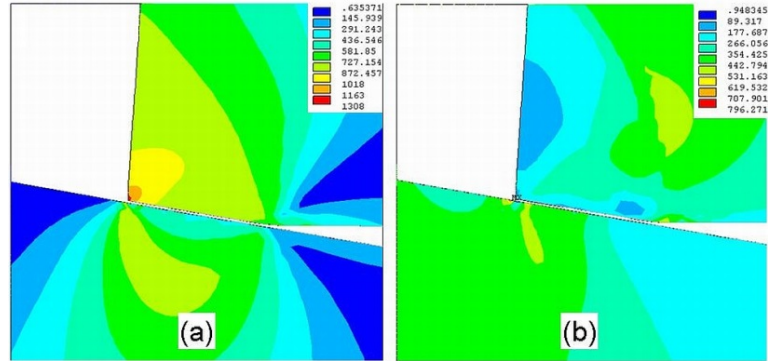


Fig. 6. Stress  $\sigma_{eq}$  under: (a) only the assembly force  $F = 184$  kN; (b) additional operating loading  $p = 250$  MPa (lens-ring-gasket)

The distribution of equivalent stress  $\sigma_{eq}$  for the assembly interference  $\delta = 1.0\%$  under the operating load  $p = 100$  MPa at the contact surfaces of the wave-ring gasket and the seat is depicted in Fig. 5. The results of numerical calculations of the equivalent stress  $\sigma_{eq}$  in the contact region of the lens-ring gasket are shown in Fig. 6a for the joint subjected to the assembly force  $F = 184$  kN only, and in Fig. 6b for the closure subjected to the additional operating pressure  $p = 250$  MPa.

The interference fits  $\delta$  between the wave-ring gasket and both sectional seats are arranged in numerical calculations by means of the *thermal method* (FEM 1) and applying the *force in principle method* (FEM 2). For the calculation purpose, the gasket was cooled down and after inserting into the seats and expanding, the appropriate interference fits were obtained in the closure in the first case. The thermal simulation of the assembly process leads to the symmetric results in both half-parts of the axial cross-section. The second numerical approach follows the assembly process performed on the stand during the experiment. The gasket was pressed into the bottom sectional seat and next the upper seat was pressed down until the edges of both seats have in touch. In this case, the symmetry of results with respect to the middle surface disappears.

The *Coulomb dry friction* in contact zones is included in the proposed finite element models with the coefficient of friction  $\mu = 0.25$  assumed for the wave-ring gasket and  $\mu = 0.40$  assumed for the lens-ring gasket [2, 5].

## 5. Comparison of analytical approach, FEM simulation and test results

The detailed analytical and numerical calculations are carried out for the dimensions of the gaskets, which were applied in [2, 5]. With respect to experimental tests the wave-ring gasket (Fig. 1b) is described by  $\varnothing A = 125$  mm,  $\varnothing C = 105$  mm,  $R_1 = 14$  mm,  $2h = 20$  mm and  $2l = 35$  mm. In the analytical approach the thickness  $t = 8.73$  mm of the gasket is assumed which is the arithmetic mean of three extreme values in the cross-sections of coordinates  $x = 0$ ,  $h$  and  $l$ . The radius  $r = 56.87$  mm results from the thickness  $t$  and from the radius  $\varnothing A/2$  of the seat. Moreover, it is assumed that the seats are executed in the walls of maximum admissible thickness ratio  $\beta = 2$ .

The *dimensionless variables* are introduced to investigate the strength and operating properties of the wave-ring gasket. The strength in the cross-section  $x = 0$  is analysed using the parameter  $\sigma = \sigma_{eq}/R_{0.2g}$ , where  $R_{0.2g}$  stands for the yield point of the gasket material. The practical recommendations are applied to verify the leak tightness of the joint. It is assumed that the closure

is leak-proof if the average contact pressure  $q_{m\text{ opr}} > R_{0.2\text{ g}} > 2p$ , where because of the strongly simplified assumptions  $q_{m\text{ opr}} = 2q_{\text{max opr}}/3$  due to the *parabolic elastic Hertz distribution*. The leak tightness parameter  $\psi = q_{m\text{ opr}}/2p$  is then introduced to investigate the functional quality of the joint. The dimensionless operating pressure is defined as  $\tau = p/R_{0.2\text{ g}}$ . Another dimensionless variables subjected to change in the analysis are defined as:  $\chi = t/h$ ,  $\delta$  – relative radial interference (in per miles),  $\gamma = t/r$  and  $\rho = R_1/t$ , where all the quantities are defined in Figs. 1b and 3.

The analysis is based on the variation of one of the introduced parameters  $\chi$ ,  $\delta$ ,  $\gamma$  and  $\rho$  in the technically acceptable range while the remaining parameters are kept at a constant mean level. Dimensionless geometry ratio varies in the range  $\chi = 0.06 - 1.60$ , radial interference is changed in the range  $\delta = 0.5\text{ ‰} - 3.0\text{ ‰}$ , dimensionless average thickness is modified in the range  $\gamma = 0.05 - 0.30$  and dimensionless radius of the working wave surface is subjected to variation in the range  $\rho = 0.5 - 3.0$ . The mean values of dimensionless parameters refer to the geometry of the closure used in the experimental investigations:  $\chi = 0.8730$ ,  $\delta = 1.0\text{ ‰}$ ,  $\gamma = 0.1535$  and  $\rho = 1.6037$ .

The ratio of cross-sectional dimensions  $\chi$  has a distinct influence on the strength of the gasket. The examination of the relationship in Fig. 7 leads to the conclusion that an increase of  $\chi$  from 0.6 to 1.6 results in a significant increase of the gasket load capacity  $\tau$ . It is assumed that because of the highly approximate assumption of the stress distribution in the contact region, the leak tightness is preserved for the parameter  $\psi \geq 2$ . The average stress  $q_m$  calculated on the basis of purely elastic Hertz approach is in this case four times greater than the applied operating pressure  $p$ . The variation of  $\rho$  connected with the working surface of the gasket produces significant changes in the leak tightness parameter  $\psi$  (Fig. 8). Too high value of this parameter ( $\rho > 3.0$ ) may be the cause of a loss of leak tightness, in particular for greater values of the operating pressure  $\tau$ .

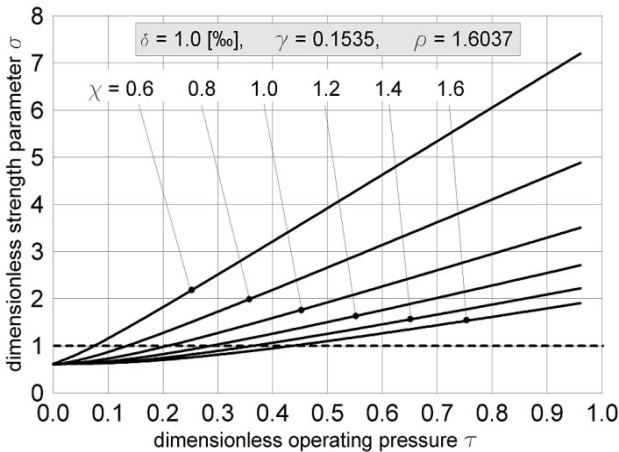


Fig. 7. Parameter  $\sigma$  versus operating pressure  $\tau$  for different  $\chi$ . Parameters  $\delta$ ,  $\gamma$  and  $\rho$  at average values

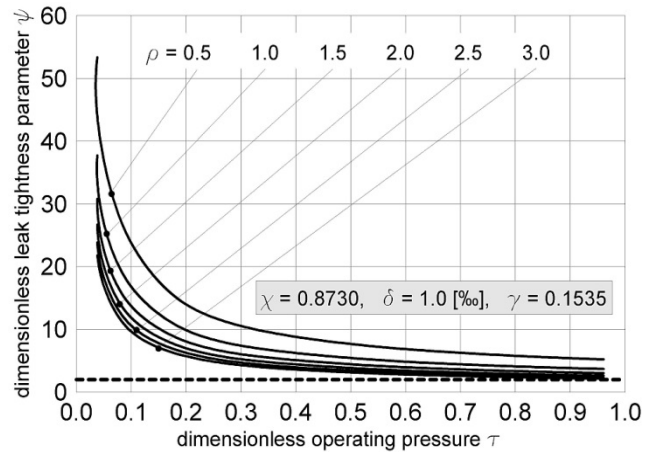


Fig. 8. Parameter  $\psi$  versus operating pressure  $\tau$  for different  $\rho$ . Parameters  $\chi$ ,  $\delta$ , and  $\gamma$  at average values

Examination of the strength parameter  $\sigma$  distributed along the gasket width (Fig. 9) confirms that application of the numerical model FEM 2, similar to real test conditions, makes the numerical results closer to the test results, in particular for the small nominal radial interference  $\delta = 0.5\text{ ‰}$ . Most of the test results are placed in the vicinity of the range received by FEM 2 method and the analytical approach. Application of greater interferences  $\delta$  (1.0 ‰ and 2.0 ‰) results in respectively greater differences between FEM 1 and FEM 2 methods and the analytical solutions, whereas the test results are located between FEM 1 and analytical results. The FEM 1 method is overestimated and analytical calculations are underestimated with respect to the experiment.

The strength of the lens-ring gasket is investigated using the appropriate parameter defined as  $\sigma = \sigma_{eq}/R_{0.2\text{ s}}$ , where  $R_{0.2\text{ s}}$  stands now for the yield point of the seat material. The dimensionless coordinate is referred to the width of lens-ring gasket  $\xi = x/h_w$  and two other parameters are

introduced:  $\omega = q/R_{0.2s}$  and  $\zeta = s/(r + t/2)$ , where the origin of  $s$  axis coincides with the internal shifted edge of the gasket. The analytical and FEM calculations are presented in Fig. 10 for the assembly force  $F = 200$  kN. They are compared with test results. The experimental investigations are carried out for the gaskets of the same extreme radii  $r - t/2 = 20$  mm,  $r + t/2 = 30$  mm and  $r_s = 22.5$  mm but of different width  $2h_i = 12.5$  mm and 25 mm (Fig. 2b and 4). The maximum values of  $\sigma$  obtained in FEM modelling and in the analytical approach are overestimated with respect to the test results on 40% and on 69%, respectively, for the gasket of smaller width. The differences are less for the gasket of greater width – 34% and 61%, respectively. The equivalent stress calculated additionally using the thick-walled model is less on 34% and 27% with respect to the test results.

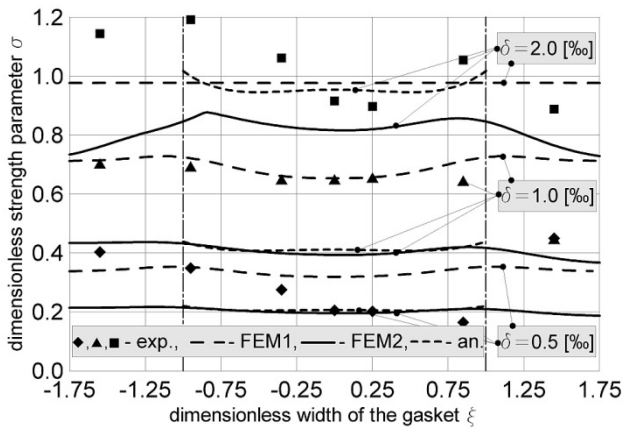


Fig. 9. Parameter  $\sigma$  for the wave-ring gasket versus  $\xi$  in assembly conditions ( $\tau = 0$ ) for the assembly interferences  $\delta = 0.5, 1.0$  and  $2.0\%$

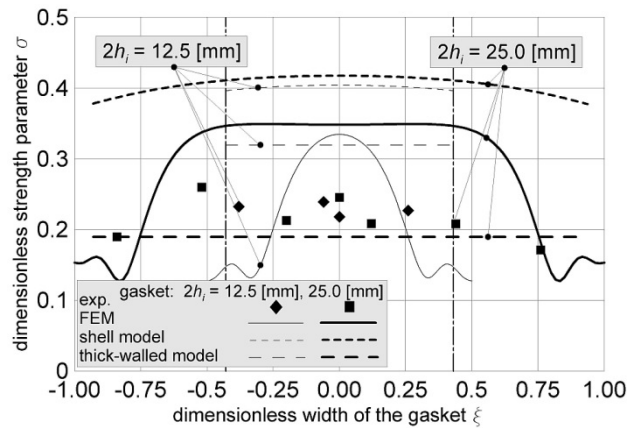


Fig. 10. Parameter  $\sigma$  for the lens-ring gasket versus  $\xi$  in assembly conditions ( $F = 200$  kN,  $\tau = 0$ ) for the gasket depth  $2h_i = 12.5$  and  $25.0$  mm

The practical approach connected indirectly with the regulations of the *Office of Technical Inspection* (OTI) is usually applied in design projects of the lens-ring gaskets. The effective width  $U_{efpr}$  of the gasket, which ensures the leak tightness of the joint, must be known in advance. The original OTI procedure used in calculations of compression load on the flat metal gaskets is misleading because of the small width of the contact region existing in lens-ring gaskets. The minimum seating pressure  $\sigma_r$ , being a function of external calculation pressure  $p_o$ , exceeds several times the yield point  $R_{0.2s}$  of the seat as the pressure  $p_o$  reaches several hundred MPa. The practical assembly force  $F_{pr}$  is then determined using the pressure  $\sigma_r$  equals to the yield point  $R_{0.2s}$ .

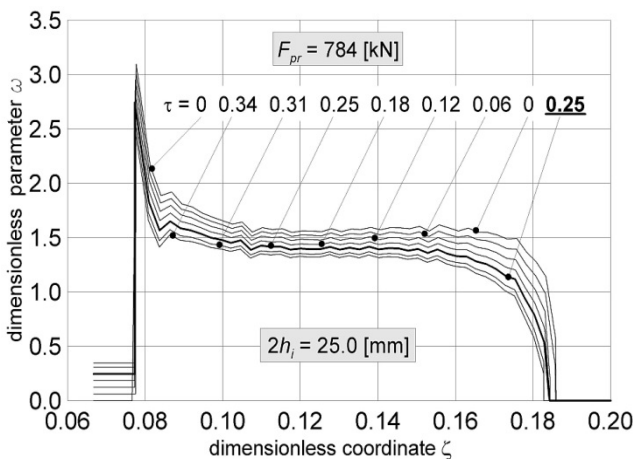


Fig. 11. Parameter  $\omega$  at the contact region of the lens-ring gasket versus  $\zeta$  under the loading  $F_{pr} = 784$  kN

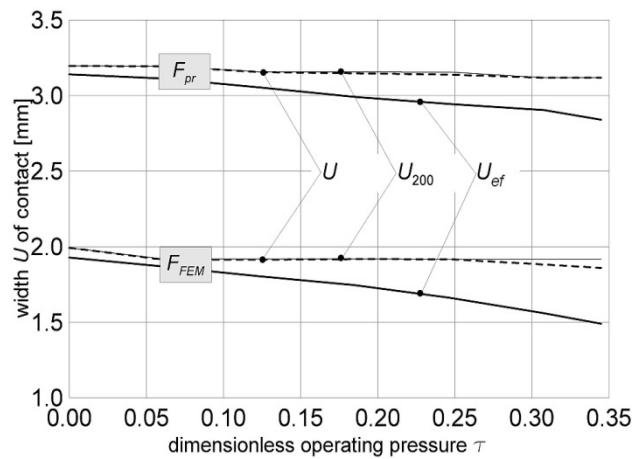


Fig. 12. Width  $U$  at the contact region of the lens-ring gasket versus  $\tau$

The geometry and materials of investigated lens-ring gasket and seat are similar to those applied in the heavy-duty reactor designed for the calculation pressure  $\tau_o = 0.3446$  ( $p_o = 280$  MPa). Assuming practical value  $U_{efpr} = 1.5$  mm the assembly force  $F_{pr} = 784$  kN, while blind application of the OTI code leads to the assembly force  $F_{OTI} = 1\ 454$  kN. The distribution of the dimensionless compression  $\omega$  at the contact region versus the dimensionless coordinate  $\zeta$  is presented in Fig. 11 for  $F_{pr} = 784$  kN and  $2h_i = 25.0$  mm. The numerical calculations are carried out with respect to the real procedure of starting the installation, which assumes first loading to the calculation pressure  $\tau_o$ , next completely unloading and eventually repeated loading to the operating pressure  $\tau$ .

The comparison of the width  $U$  of the contact region versus operating pressure is depicted in Fig. 12 for different values of the assembly force. Numerical analysis of this leak parameter is carried out for  $F_{pr}$  and for  $F_{FEM} = 460$  kN, for which FEM calculations lead to the practical value  $U_{efpr} = 1.5$  mm. Examination of presented relationships reveals that for  $F_{pr}$  and under the loading  $\tau_o$  the gasket effective width  $U_{ef}$  is nearly twice greater as the initially assumed one. The above remark leads to the conclusion that the closure is probably unnecessarily overloaded.

## 6. Final remarks

The obtained results lead to certain general conclusions and recommendations with respect to the safety of the considered joints.

The strength of a wave-ring gasket cannot be improved significantly through the change of parameter  $\gamma$ , however, greater loading capacity may be obtained through an increase of  $\chi$ . Special attention should be paid to the initial assembly interference fit  $\delta$ . The interference  $\delta < 0.5$  ‰ may cause leakage of the installation at the start. On the other hand,  $\delta > 2.5$  ‰ appears to be too large, because it produces critical damage of relatively soft working surfaces during the assembly.

Specific geometric features of the joint with the lens-ring gasket cause that the strength of the closure can be easily obtained. With respect to its strength, the gasket is usually strongly oversized. The actual problem is to ensure the required leak tightness applying appropriate assembly force  $F$ .

The analytical computational models of the joints may be convenient to proceed an initial analysis. A large number of simple calculations can be carried out for different geometry of the gaskets, different material properties and assembly requirements. It should be noted, however, that analytical calculations are in general underestimated with respect to the test. The final parameters of the closure may be then determined in the detailed expensive and time-consuming FEM verifications, which lead to the results closer to the experimental results.

## References

- [1] Krasinski, M., Trojnacki, A., *Computational model of metal high-pressure 2-delta gasket*, Technical Transactions, 3-M/2009, pp. 31-58, 2009.
- [2] Krasinski, M., Trojnacki, A., *Experimental investigations of metal high-pressure "2-delta" gasket*, The Archive of Mechanical Engineering, Vol. LVII, No. 4, pp. 355-381, 2010.
- [3] Ryś, J., Szybiński, B., Trojnacki, A., *Computational model of metal high-pressure wave-ring gasket*, Technical Transactions, 11-M/2006, pp. 63-87, 2006.
- [4] Stein, E., *Error-controlled adaptive finite elements in solid mechanics*, John Wiley&Sons, Ltd, West Sussex 2003.
- [5] Szybiński, B., Trojnacki, A., *Analytical and numerical solutions of metal high-pressure wave-ring gasket*, The Archive of Mechanical Engineering, Vol. LXII, No. 1, pp. 19-44, 2015.
- [6] Trojnacki, A., *Druckstandfestigkeit und Betriebseigenschaften von Doppelwellendichtungen*, Chemie Ingenieur Technik, Vol. 83, No. 3, pp. 377-385, 2011.
- [7] Wriggers, P., *Computational contact mechanics*, John Wiley&Sons, Ltd, West Sussex 2002.
- [8] Życzkowski, M., *Technical Mechanics, Vol. IX. Strength of materials*, PWN, Warsaw 1988.